EXTRACTION OF EAC CRACK GROWTH RATES AND STRESS INTENSITY FACTORS FROM SLOW STRAIN RATE TESTS DATA FOR 5XXX AND 7XXX SERIES ALUMINUM ALLOYS

Henry Holroyd, Bolivar, USA
henry.holroyd@luxfer.net

A knowledge of crack propagation rate as a function of the applied stress intensity factor (K) to generate crack velocity-K (cv-K) curves for aluminum alloys is desired due to their propensity for environment-assisted cracking (EAC). However, to do this has historically required the use of standard fracture mechanics test specimens requiring several days to months per test. In addition, most data obtained in this way involves the use of fixed-displacement double-cantilever-beam (DCB) or compact-tension-specimens (CTS). Here, the applied K during testing decreases with increasing EAC crack length, and the K-factor measured at the end of testing is a 'crack arrest' parameter, as opposed to an EAC threshold factor, K_{1SCC} as assumed in most studies, which may become invalidated by crack branching and in some environmental conditions by secondary stresses generated in the crack-tip region due to local wedging from corrosion products.

A method of extracting information to construct EAC crack velocity-K curves under raising load (and K) conditions from slow strain rate test taking only a few hours is provided. Verification of assumptions made with regards to EAC crack initiation and growth is presented based on 3D computed Tomography data from interrupted slow-strain rate tests and information from 4D computed Tomography data from slow-strain rate experiments conducted on the Diamond Light Source Synchrotron.

RECOMMENDATIONS AND RANTS REGARDING RESEARCH ON ENVIRONMENTALLY ASSISTED CRACKING

Stanley Lynch, Monash University, Australia
lynch_stan@hotmail.com

Controversies concerning mechanisms and kinetics of environmentally assisted cracking seem to be increasing despite (or because of?) the accumulating numbers of papers and the increasing capabilities of techniques used to study the phenomena. My presentation will discuss the approaches and experiments that I would like to see undertaken (given that I have 'retired' and do not have the resources or students to carry them out) to address this unsatisfactory state of affairs. I will also address some of the misunderstandings and misconceptions regarding mechanisms of environmentally assisted cracking that have appeared in the recent literature. A primary recommendation (and plea) is for more studies of liquid-metal embrittlement (LME) (in systems involving only adsorption at crack tips) since this type of LME is the least complex case of environmentally assisted cracking, and there are still many aspects that are not well understood (as will be outlined). More studies of LME would provide a better basis for understanding the more complex phenomena of hydrogen embrittlement (HE) and stress-corrosion cracking (SCC), as previous studies have demonstrated to some extent. Using single crystals and bi-crystals as well as studying complex commercial alloys would obviously be a logical approach. One of the common misconceptions regarding environmentally assisted cracking (in my opinion) is that hydrogen-assisted cracking (when hydrides are not involved) occurs primarily by hydrogen enhanced localised plasticity (HELP) involving solute hydrogen facilitating dislocation activity in the plastic zone ahead of cracks, and I will discuss why I think that this view is misconceived. The adsorption-induced dislocation emission (AIDE) mechanism for some HE and LME systems is supported by numerous observations, but is often misunderstood (judging by the discussions in a recent conference proceeding [1]), and clarifications will be provided.

[1] The challenges of hydrogen in metals, Philos. Trans. Roy. Soc. A, Vol. 375, July,2017, T. Paxton, A.P. Sutton, and M.W. Finnis (Eds).

UNIFIED APPROACH TO CRACK GROWTH AND FRACTURE

K. Sadananda, Technical Data Analysis Inc., 3190 Fairview Park, Falls Church, VA 22043, USA
kuntimaddisada@yahoo.com
M. Nanibabu, Metallurgy and Materials Group, Materials Development Technology Division, Indira Gandhi Centre for Atomic Research, India
A.K.Vasudevan, Technical Data Analysis Inc., 3190 Fairview Park, Falls Church, VA 22043, USA

Unified approach connects the behavior of a smooth specimen, of a notched specimen and of the fracture-mechanics specimen, under inert and corrosive environments, using the unifying principles and the Modified Kitagawa-Takahashi Diagram. The unifying principles are based on the fact that the behavior of short cracks is not different from that of long cracks, and the same thresholds govern the crack growth. Cracks being high energy defects, local internal stresses are required to initiate and grow the cracks in all cases. The internal stresses can be pre-existing as in the case of long cracks or in situ generated or augmented in the case of smooth and notched specimens. Observed variations in the crack growth rates of short cracks from those of long cracks arise due to variations in the types and degrees of pre-existing internal stresses. In aggressive environments, chemical forces provide additional driving forces over and above the mechanical forces. Chemical forces come from the chemical and/or electro chemical potential gradients which may be difficult to determine as they depend on the nature and the extent of the local chemical reactions in the changing compositional gradients. From practical considerations, we show that they can be quantified using the inert medium as a reference. Cyclic loads provides additional factors since crack tip driving forces come from both monotonic and cyclic loads leading to load-ratio R dependence. We provide here a systematic analysis of these factors using our Unified Approach to help in quantification and codification of the kinetics of the crack growth and fracture.

DO CORROSION PITS ELIMINATE THE BENEFIT OF SHOT-PEENING?

Alan Turnbull, National Physical Laboratory
alan.turnbull@npl.co.uk
Shengqi Zhou, National Physical Laboratory
Louise Crocker, National Physical Laboratory

Key Words: pits, shot peening, fatigue limit, fatigue crack growth.

Shot peening is used in many industrial applications, e.g. steam turbine blades, to induce near-surface compressive residual stresses and reduce the likelihood of failure by fatigue, corrosion fatigue and stress corrosion cracking. On the whole, shot peening has proven to be very successful in increasing the life of structures and components. However, the depth of the compressive stress layer is typically only about 250 µm and this poses the question as to the retained benefit when corrosion pits develop to varying depth. In the first stage to addressing this issue we show that the fatigue limit of a 12 Cr martensitic stainless steel turbine blade material tested in air at varying pit depths, ranging from 50 µm to 320 µm, was still significantly enhanced by shot peening even for the maximum depth studied. Complementary measurement of the crack propagation rate from a corrosion pit showed that the propagation rate was retarded by the near-surface compressive stress for crack depths up to 0.9 mm, well beyond the depth of the compressive layer. Serial sectioning to identify the loci of crack initiation sites yielded the unexpected result that crack development occurred preferentially away from the pit base, especially for the smaller pit depths. Finite element analysis to predict the stress and strain around a corrosion pit and to estimate the stress intensity factor will be described as a basis for rationalising the experimental observations.

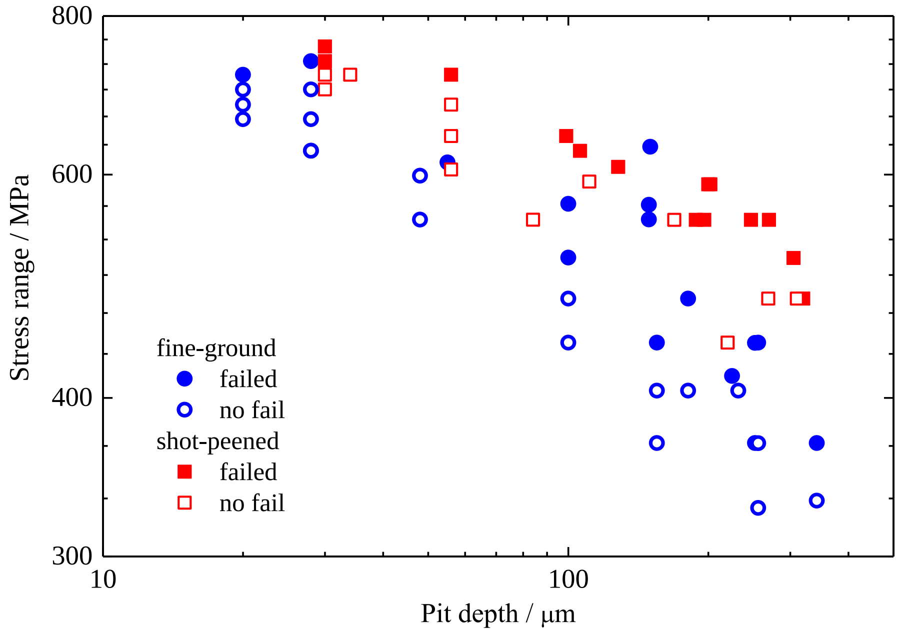

Figure 1. Effect of pit depth on the fatigue strength at 10^7 cycles for fatigue crack initiation from pits in fine-ground (stress-relieved) and shot-peened blade steel surface in air at 90 °C; R=0.1; Frequency = 35 Hz.

INITIATION AND GROWTH OF CORROSION-FATIGUE CRACKS FROM CORROSION PITS USING ELASTIC-PLASTIC NOTCH ANALYSIS

K. Sadananda, Technical Data Analysis Inc., USA
kuntimaddisada@yahoo.com
M. Amiri, Technical Data Analysis Inc., USA
A.K. Vasudevan, Technical Data Analysis Inc., USA

Corrosion pits are known to act as precursors for fatigue crack initiation under corrosive environment. The transition from pit to crack growth under corrosion fatigue is of considerable interest for many engineering structures. Several predictive methodologies have been developed. As the Pits grow with large aspect ratio, they behave like local stress/strain concentrations accentuating the crack initiation and growth. In this paper, we extend our recent analysis of crack initiation at the elastic-plastic notch tip stress fields* to evaluate its applicability to pit to crack transition.

Ref: K. Sadananda, A. Arcari, A.K. Vaudevan, Eng. Frac. Mech., 2017, 176 pp.144-160

WHEN DO SMALL FATIGUE CRACKS PROPAGATE AND WHEN ARE THEY ARRESTED?

Stefanie E. Stanzl-Tschegg, University of Natural Resources and Life Sciences, BOKU Vienna
Stefanie.tschegg@boku.ac.at

Key Words: corrosion fatigue, defect sizes, loading frequency, R-ratio, steels.

Mainly the role of the following parameters is treated:

- material (steels, Al-alloys, Cu – heat treatment),
- kind of loading (stress range, R-ratio, mode I, mixed mode loading, constant and variable amplitudes, 10 Hz, 20 kHz)
- environment (vacuum, humid air at 20 °C, dry air at 90 °C, aqueous solution with different Cl^--concentration,
- initial defect size (small-crack length, voids, inclusions, corrosion-pit size, PSBs),

Different evaluation procedures were developed, and for a better understanding of the relevant mechanisms. Initiation and growth of small and long cracks were measured. The results are correlated with microscopic surface observations, and SEM fracture analysis is used for a quantification of crack initiation, propagation and arrest mechanisms. The two-parameter model of Vasudevan and Sadananda is applied besides other models (Kitagawa-Takahashi, El Haddad) for realistic life-time predictions. They help to reduce costs for extensive tests and also material and thus weight of machine parts and constructions.

CA	Rough crack surfaces, deep secondary cracks	→	Arrest of small cracks
VA	Flatter crack surfaces and less deep secondary cracks due to many periodic overloads	→	Growth of small cracks with initial rate > $1,7x10^{-12}$ m/c

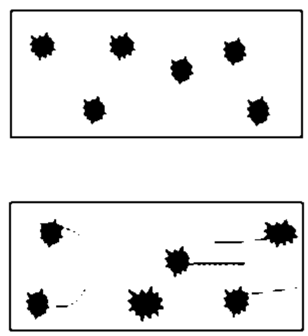

Figure 1 – Role of crack surface roughness on growth of small cracks at CA and VA fatigue loading

SHORT CRACK TOLERANCE UNDER EAC CONDITIONS

JTP Castro, Mechanical Engineering Department, PUC-Rio, Brazil
jtcastro@puc-rio.br
RV Landin, Mechanical Engineering Department, PUC-Rio, Brazil
IN Viçosa, Mechanical Engineering Department, PUC-Rio, Brazil
GR Altoé, Mechanical Engineering Department, PUC-Rio, Brazil
RRC Saúde, Mechanical Engineering Department, PUC-Rio, Brazil

Notch sensitivity effects under environmentally-assisted cracking (EAC) conditions have been recently quantified considering the tolerance to short cracks that may start at their tips and become non-propagating after growing for a while, a behavior that depends on the stress gradients ahead of the notch tips and on the basic material resistances to crack initiation (S_{EAC}) and propagation (K_{IEAC}) inside an aggressive medium under static loadings. Such properties are time-independent, so they can be directly compared with the notch gradient-affected stress intensity factors of the short cracks that depart from notch tips. This model can provide a powerful alternative design tool for the pass/non-pass criterion traditionally used to deal with such mechanical-chemical problems, since it properly considers and quantifies the stress analysis issues that affect them. This model has been validated by proper tests under liquid metal embrittlement conditions, and it can be used to propose a defect-tolerant design criterion under EAC conditions that includes the unavoidable notch effects always present in actual structural components.

This paper objective is to experimentally verify the proposed model predictions under other EAC mechanisms. Among them, hydrogen embrittlement (HE) is a most important one, since many catastrophic failures have been associated to it. Due to its practical importance, two different sources of hydrogen are used in this work to understand the HE short crack behavior: (1) sulfide stress corrosion (SSC) on super martensitic stainless steel in salt water with high amounts of H_2S, which produces hydrogen by a corrosive process; and (2) cathodic protection (CP) on a high strength steel in salt water, which produces hydrogen by electrolysis. In both cases, the hydrogen diffusion is slow, due to the martensitic microstructures, although high amounts of hardly-measurable hydrogen may be present around the cracking region. Since the driving force for short cracks can be associated to the stress gradient ahead of the crack tip, the SSC and CP short cracks behavior can be predicted by the same set of procedures previously qualified under liquid metal embrittlement conditions, and with under some SSC tests made with carbon steels. Moreover, a third EAC mechanism is studied in this work as well, chloride-induced cracking in austenitic stainless steels, using a boiling solution of $MgCl_2$.

ATOMISTIC MODELING OF SUSTAINED FATIGUE CRACK GROWTH UNDER REALISTIC CONDITIONS

Derek Warner, Cornell University
derek.warner@cornell.edu

Key Words: fatigue, fracture, atomistic modeling, dislocations, metals

This presentation will review the Cornell Fracture Group's effort to apply modern atomistic based simulation techniques to advance the mechanistic understanding and models of fatigue crack initiation in naval aviation. The overall effort is aimed at (1) bridging the gap between existing fatigue initiation models and real-world service conditions, (2) providing mechanistic based material separation rules for microstructural models, and (3) identifying nanoscale routes for improved fatigue performance/mitigation via new alloys, coatings, and/or treatments. Broadly, improved fatigue prediction capabilities may translate to fewer unexpected failures, decreased ownership costs, and the increased availability of existing aircraft.

Observations of fatigue cracks emanating from material defects such as corrosion pits are very common; yet, one can argue that fatigue crack nucleation and subsequent growth has never been predicted in a fundamental model (i.e. ab-initio or even atomistic). Over the past decade, the Cornell Fracture Group has worked in this area, focusing primarily on the crack-tip chemomechanics associated with environmental effects. More recently, the group has been directing its attention towards the more fundamental question of what conditions make sustained fatigue crack growth possible. This presentation will discuss the hypotheses that we have made, the subsequent test simulations/model that have been performed, and the conclusions that can be drawn.

INTERGRANULAR CORROSION AND GRAIN DISSOLUTION WITH PERIDYNAMICS

Florin Bobaru, University of Nebraska-Lincoln, USA
fbobaru2@unl.edu
Siavash Jafarzadeh, University of Nebraska-Lincoln, USA
Ziguang Chen, Huazhong University of Science and Technology, China

Key Words: Corrosion damage, peridynamics, intergranular corrosion, stress-dependent corrosion.

In polycrystalline material, intergranular corrosion (IGC) is a major cause for failure initiation and leads to significant reduction in strength. The sharp and narrow defects along grain boundaries induced by the corrosion damage along grain boundaries act as stress concentration sites, from which cracks can easily develop. While progress has been made on certain aspects of modeling IGC damage, it can be said that a fully predictive model is no yet available. In this work, we introduce a peridynamic (PD) model (see [1] and [2]) for IGC damage ([3]). We use mixed potential theory and mass transfer in the electrolyte to model IGC. The model considers different dissolution rates for grains and grain boundaries based on their corresponding Tafel kinetics. We validate our model quantitatively against published experiments for IGC in a AA2024 foil immersed in NaCl solution. In addition, we show that new PD model can successfully capture the combination of grain boundary corrosion and grain dissolution at higher potential values (see Fig. 1), in agreement with experimental observations. We extend the model to treat general micro-galvanic corrosion and compare our results with experimental ones.

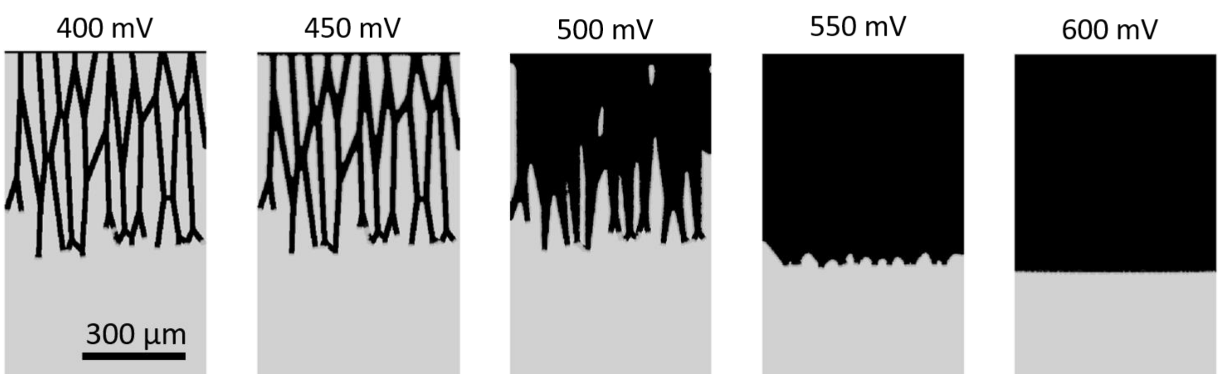

Figure 2 – Peridynamic simulations (sample morphology) for corrosion of AA2024-T3 sheet exposed to 1M NaCl solution in L-direction for 4 hours at different applied potentials.

References

[1] Chen, Z., & Bobaru, F. (2015). Peridynamic modeling of pitting corrosion damage. Journal of the Mechanics and Physics of Solids, 78, 352-381.

[2] Jafarzadeh, S., Chen, Z., & Bobaru, F. (2018). Peridynamic modeling of repassivation in pitting corrosion of stainless steel. CORROSION, in print.

[3] Jafarzadeh, S., Chen, Z., & Bobaru, F. (2018). Peridynamic modeling of intergranular corrosion damage (in review).

BUILDING ENVIRONMENTAL HISTORY FOR NAVAL AIRCRAFT

William C. Nickerson, Office of Naval Research, Arlington, VA 22203, USA
william.nickerson@navy.mil
Mehdi Amiri, Technical Data Analysis Inc., Falls Church, VA
Nagaraja Iyyer, Technical Data Analysis Inc., Falls Church, VA

Key Words: Environmental history, Corrosion, uniform stress free corrosion, crevice corrosion, Part-specific environment and mechanical loads history, Climate builder

Operating environments of Navy aircraft vary to a good degree depending upon the squadron location, flight requirements, and other related field and ground activities. All these conditions promote both mechanical and environmental damage of various types. Uniform stress free corrosion arises from the geographical location ambient weather and the average ground time of the aircraft. Even a small scratch during operation can lead to a corrosion cell arising under a surface moisture film. Use of de-icing salts in cold environments will also accelerate the corrosion process. Crevice corrosion, meanwhile, results from the accumulation of dirt and debris in confined spaces such as access door flanges and wheel wells; as well as capillary action that keeps faying surfaces wetted even in low humidity exterior conditions. Due to the presence of wet condensates and appreciable concentrations of chloride (and other active) ions, many areas of the aircraft are prone for pitting, intergranular attack or exfoliation. The aircraft operations will also have influence on type and morphology of corrosion. Thus, building an environmental history of the aircraft is crucial to correctly identify different corrosion and mechanical damage processes to monitor and track the development of attack in many areas of the aircraft structure.

We outline a method for building the environmental history of Naval aircraft using three available resources: maintenance and materials management (3M) system data, daily weather history data of the squadron location, and field activity data as recorded in logbooks. This includes development of a part-specific microclimate builder which tracks a local climate history specific to a part or component. The climate builder takes the flight information such as flight duration, altitude, geographical location, etc., as well as daily weather history data from the NOAA Database. It will translate the asset service history (such as: stored indoors vs. outdoors) into a series of scenarios and assigns weighting factors to these scenarios based on geographical location. The underlying approach that is currently used in the climate scenario builder is based on both models/simulations and sensor data. Our current suite of models combined with the climate builder will provide an integrated framework within which life prediction for a combinatorial situation of mechanical and environmental history can be performed.

HYDROGEN EFFECTS ON MECHANICAL PERFORMANCE OF NODULAR CAST IRON

Hannu Hänninen, Aalto University School of Engineering, Dept. of Mechanical Engineering, Finland
hannu.e.hanninen@aalto.fi
Antti Forsström, Aalto University School of Engineering, Dept. of Mechanical Engineering, Finland
Yuriy Yagodzinskyy, Aalto University School of Engineering, Dept. of Mechanical Engineering, Finland

The ferritic nodular cast iron grade EN-GJS-400-15 intended for use as the load-bearing part of canisters for long-term disposal of spent nuclear fuel was studied in order to evaluate its sensitivity to the hydrogen-induced effects on mechanical performance. Hydrogen was introduced in the cast iron electrochemically from 1N H_2SO_4 solution under controlled cathodic potential. Hydrogen uptake in the course of tensile testing was measured using hydrogen thermal desorption method. It was found that plastic deformation of the specimens in the continuous hydrogen charging results in a remarkable increase of hydrogen uptake in the studied cast iron.

Constant extension rate tests (CERT) and constant load tests (CLT) performed under continuous electrochemical hydrogen charging showed a remarkable reduction of elongation to fracture in CERT and time to fracture in CLT as compared to the corresponding values obtained by testing in air and water environments. The most important finding is that hydrogen increases dramatically the creep rate of the cast iron in CLT already at applied load of about 0.5 x yield stress. The tensile tests were followed with SEM observations of the hydrogen-induced cracking appearance on the tensile specimen outer and fracture surfaces.

The obtained results are discussed in terms of the specific role of the graphite nodules as abundant sources of hydrogen and the nodule distribution in the cast iron matrix in the mechanisms of hydrogen-induced cracking.

ELUCIDATING THE MECHANISTIC INFLUENCE OF STRENGTHENING PRECIPITATE MORPHOLOGY ON HYDROGEN ENVIRONMENT-ASSISTED CRACKING IN A NI-CU SUPERALLOY

Zachary D. Harris, University of Virginia, Charlottesville, VA, USA
zdh8kt@virginia.edu
James T. Burns, University of Virginia, Charlottesville, VA, USA

Key Words: nickel-based superalloys, dislocations, HEAC, localized deformation, hydrogen embrittlement

Recent studies on Ni and Fe-based alloys utilizing transmission electron microscopy (TEM) of the near-fracture surface region have revealed a systematic refinement in the dislocation cell structure of hydrogen-charged specimens relative to non-charged specimens. These observations suggest that hydrogen-induced localization of deformation may provide an important contribution to the microscale processes by which hydrogen degrades the performance of structural metals. Moreover, this finding implies that microstructural features which affect deformation processes could be tuned so as to increase an alloy's intrinsic resistance to hydrogen-induced degradation. For example, given the dominant influence of strengthening precipitates on deformation processes in precipitation-hardened alloys, it is hypothesized that such particles could be optimized to mitigate this hydrogen-induced localized deformation. However, studies which evaluate the role of precipitate morphology on these localized deformation processes in the context of hydrogen-induced cracking are limited in number and often complicated by the simultaneous influence of other microstructural features.

This study seeks to remedy this knowledge gap by examining the role of strengthening precipitate morphology on the hydrogen environment-assisted cracking susceptibility of a model precipitation-hardened alloy. First, Monel K-500 was systematically heat-treated so as to produce strengthening precipitate (γ' (Ni_3Al)) sizes which result in distinct global slip behavior. Evaluated heat treatments corresponded to the non-aged (no γ'; wavy slip), under-aged (small γ'; planar slip via particle shearing), peak-aged (medium γ'; mixed), and over-aged (large γ'; wavy slip via Orowan looping) conditions. TEM of each heat treatment condition confirmed the presence of the targeted precipitate/slip morphologies; the absence of strengthening precipitates in the non-aged alloy was also corroborated by X-ray diffraction experiments. Second, the effect of precipitate morphology on HEAC metrics was assessed through slow-rising stress intensity (K) testing in dry N_2 gas and 0.6 M NaCl solutions under applied potentials of -1000, -1100, and -1200 mV_{SCE}. Testing revealed a systematically decreased HEAC susceptibility for the non-aged and over-aged conditions relative to the under-aged and peak-aged conditions, suggesting that HEAC susceptibility is increased in alloys which exhibit planar slip. Third, a detailed microstructural characterization effort was completed to ensure that this difference in HEAC behavior is predominantly attributable to the variations in precipitate morphology. Microstructural features which may vary with applied isothermal ageing heat treatment are (1) grain size, (2) grain boundary character, (3) grain boundary impurity concentrations, and (4) precipitate morphology. Electron backscatter diffraction (EBSD) showed minimal changes in grain size and grain boundary character distribution between the four tested conditions, confirming that such variables are not responsible for the observed variations in HEAC susceptibility. Auger electron spectroscopy (AES) revealed a systematic enhancement in the grain boundary sulfur concentration with increased ageing time. However, the increased resistance of the over-aged alloy relative to the under-aged and peak-aged conditions implies that grain boundary sulfur concentration is not responsible for the measured differences in HEAC susceptibility.

Taken together, these results demonstrate the potent role of precipitate strengthening morphology on HEAC susceptibility, suggesting that such microstructural features can be optimized to improve an alloy's intrinsic resistance to HEAC. Variations in precipitate morphology are expected to affect HEAC through changes in hydrogen trapping behavior and bulk slip morphology. Given that hydrogen trapping in Monel K-500 was previously shown to vary marginally with precipitate character, these results imply a governing role of bulk slip morphology (*e.g.* planar versus wavy slip). This observed dependence of HEAC susceptibility on bulk slip morphology motivates the re-examination of micromechanical models of HEAC metrics which assume a specific slip geometry. Possible model modifications to account for these new results are discussed and future experiments to further explore the mechanistic implications of this dependence on bulk slip morphology are proposed.

DUCTILE-BRITTLE TRANSITION TEMPERATURE SHIFT CONTROLLED BY GRAIN BOUNDARY DECOHESION AND THERMALLY ACTIVATED ENERGY AND HYDROGEN GB EMBRITTLEMENT

Jun Kameda, Retired, USA
jun.kameda@gmail.com
Martin L.Jok1, independent consultant

Keywords; ductile-brittle transition temperature, grain boundary segregation and embrittlement, effects of hardness and strain rate, hydrogen embrittlement

Classical structural problems of temper embrittlement are evaluated in terms of changes in the ductile-brittle transition temperature (DBTT). Experimentally, DBTT is not only strongly dependent on the effects of the type and amount of segregated solute X_{gb}^{s} at grain boundary (GB) but also on the hardness of the steel and strain rate.

Recent first-principles calculations provide the decohesion of the GB based on the concentration of different elements on the GB. The decohesion, $2\gamma_{int}$, is difference between the energy of the fracture surfaces and the energy of the GB ($2\gamma_{int} = 2\gamma_{fs} - \gamma_{gb}$) The calculations show that the decohesion is linearly related to the concentration of metalloids on the GB. The calculations show that the embrittling potency (Δe_p) of the different metalloids, Sb, Sn, and P, are ranked as follows: $\Delta e_p^{Sb} > \Delta e_p^{Sn} > \Delta e_p^{P}$.

This study reanalyzes earlier experimental data and attempts to correlate the effect of strain rate and hardness to DBTT on samples with GB embrittled with different concentrations of Sb, Sn and P. Charpy notched and cantilever static bending tests on 3.5 Ni – 1.7 Cr steels were performed at two different strain rates and at two different hardness.

It is found that DBTT is linearly related to X_{gb} when the strain rate and hardness are not changed. That is $DBTT = c + \alpha X_{gb}$, where c and α are constants that vary with strain rate and hardness. The constant c is function related to DBTT for cleavage fracture but the slope, α, is a function of strain rate only for the medium hardness steel, but is independent of strain rate for the hard steel.

The activation energy for the motion of dislocations that is responsible for the plasticity is estimated by relating the strain rate to activation energy and DBTT through an Arrhenius relationship. This activation energy then is correlated with the $X_{gb}$and Δe_p. The activation energy is strongly dependent on GB decohesion and high hardness sample

In addition, hydrogen GB embrittlement is linked with decohesion and analyzed in terms of micro- and macro-fracture mechanics.

EFFECT OF CYCLIC LOADING ON HYDROGEN DIFFUSION IN LOW-ALLOYED CARBON STEELS

Pesenti Bucella D. Department of Engineering and Applied Sciences, University of Bergamo, Dalmine (BG), Italy
diego.pb1988@gmail.com
Cabrini M., Department of Engineering and Applied Sciences, University of Bergamo, Dalmine (BG), Italy
Lorenzi S., Department of Engineering and Applied Sciences, University of Bergamo, Dalmine (BG), Italy
Pastore T, Department of Engineering and Applied Sciences, University of Bergamo, Dalmine (BG), Italy
,

Carbon steels or low-alloyed steels may be affected by damaging phenomena due to Hydrogen Embrittlement (HE), which is a particular form of Environmental Assisted Cracking (EAC). The insurgence of HE depends on the intrinsic susceptibility of the steel, the applied stress, and the concentration of hydrogen inside the metal. It occurs by a mechanism of absorption and subsequent diffusion of atomic hydrogen through the metal lattice.

On steels with a yield strength lower than 700 MPa, HE occurs in the plastic deformation field, in the presence of dynamic loading at slow strain rates or cyclic fatigue loading at very low frequencies. Although several important studies were carried out on the effect of loading conditions on hydrogen diffusion into the metal and HE mechanism, HE phenomena are not fully understood. In this work, the effect of the application of cyclic loads on hydrogen diffusion parameters was studied both in the elastic and in the plastic deformation field. The influence of mean load and amplitude was analyzed. Hydrogen permeation tests were performed on API 5L X65 steel, in accordance with ISO 17081:2014. The specimen behaved as bi-electrode between the two compartments of a Devanathan-Stachurski cell. The anodic side of the specimen was polarized at +340 mV vs Ag/AgCl in a 0.1 M NaOH aerated solution, while the cathodic compartment was filled with an aerated borate solution. A controller enabled temperature adjustment at 20±0.5°C. Once the passivity current registered in the anodic side reached values of 0.05 $\mu A/cm^2$, a cathodic current density of 0.50 mA/cm^2 was applied to charging cathodic side. The study included tests with sine waveform cycling loading, with a maximum level equal to 110% TYS, at a frequency of 10^{-2} Hz.

The results confirmed the values of hydrogen diffusion coefficient usually indicated for low-alloyed steels with a sorbitic microstructure. Strain hardened specimens - stretched above yield strength - showed an increase of steady state current and an extension of the time lag, denoting a slight decrease in the apparent hydrogen diffusion coefficient due to traps effect in the cold deformed steel matrix.

Under cyclic loading, an instantaneous peak of current with a subsequent significant transient decrease occurred after cyclic load application, whereas no relevant variation of permeation curve compared to unloaded specimens was observed if specimens were already loaded before hydrogen charging.

The instantaneous current peak reached values much higher than the steady state current. This is ascribed to the rupture of the passive film – caused by loading – and its subsequent reformation; in fact, this can also be noted during tests performed on specimens without hydrogen permeation.

The following transient, in which the permeation current decreases below the steady state and then returns to it, denotes a relevant trapping effect that causes the instantaneous reduction of mobile hydrogen concentration in the lattice. This becomes more significant for loads closer and closer to the yield strength, mainly beyond this, and can only be noted at the first loading step. Subsequent unloading and loading step at the same mean value showed no transient in the permeation current.

EFFECT OF MECHANICAL LOADING ON THE GALVANIC CORROSION BEHAVIOR OF A MAGNESIUM-STEEL STRUCTURAL JOINT

K.N. Solanki, School for Engineering of Matter, Transport, and Energy, Arizona State University, USA
kiran.solanki@asu.edu
I. Adlakha, School for Engineering of Matter, Transport, and Energy, Arizona State University, USA
B. Gholami, School for Engineering of Matter, Transport, and Energy, Arizona State University, USA
N.C. Muthegowda, School for Engineering of Matter, Transport, and Energy, Arizona State University, USA

Keywords**:** Galvanic corrosion; Magnesium; Plastic strain; Numerical modeling study

Here a time dependent numerical model aimed to investigate the role of mechanical deformation on the corrosion behavior of galvanic joint is developed. The influence of mechanical loading on the corrosion behavior of the AE44 (Magnesium alloy) and mild steel galvanic joint immersed in a 1.6 wt% NaCl solution is explored across a wide range of combined mechanical and electrochemical conditions. It is shown that the presence of mechanical loads on the galvanic couple was found to cause an increase in both the peak and average pit depth. However, there was a noticeable increase in the peak pit depth due to the presence of plastic strain near the galvanic junction. Further, the presence of tensile loads was found to increase the tendency for localized corrosion around the galvanic junction for both the electrochemical scenarios: a) decreasing electrolyte depth; and b) larger cathodic surface area. For tensile loads greater than 60 MPa, a transition from the slow propagating corrosion pit regime (electrochemically dominated) to a rapid crack propagation (mechanically dominated) was predicted to take place within 60 hours of immersion in 1.6 wt% NaCl solution. Finally, the accumulation of equivalent strain of 3.5% ahead of the corrosion pit was found to correspond to the fracture of the galvanic joint. Overall, the findings presented here highlight the complex interactions that occur between the mechanical and electrochemical processes during stress-assisted corrosion of galvanic joints. Therefore, this systematic investigation provides a robust numerical framework for accurate examination of the role of mechanical deformation on the corrosion behavior of structural alloys. In particular, the model described here may be useful for designing, developing and ranking the structural galvanic joints that are exposed to combined mechanical and electrochemical processes.

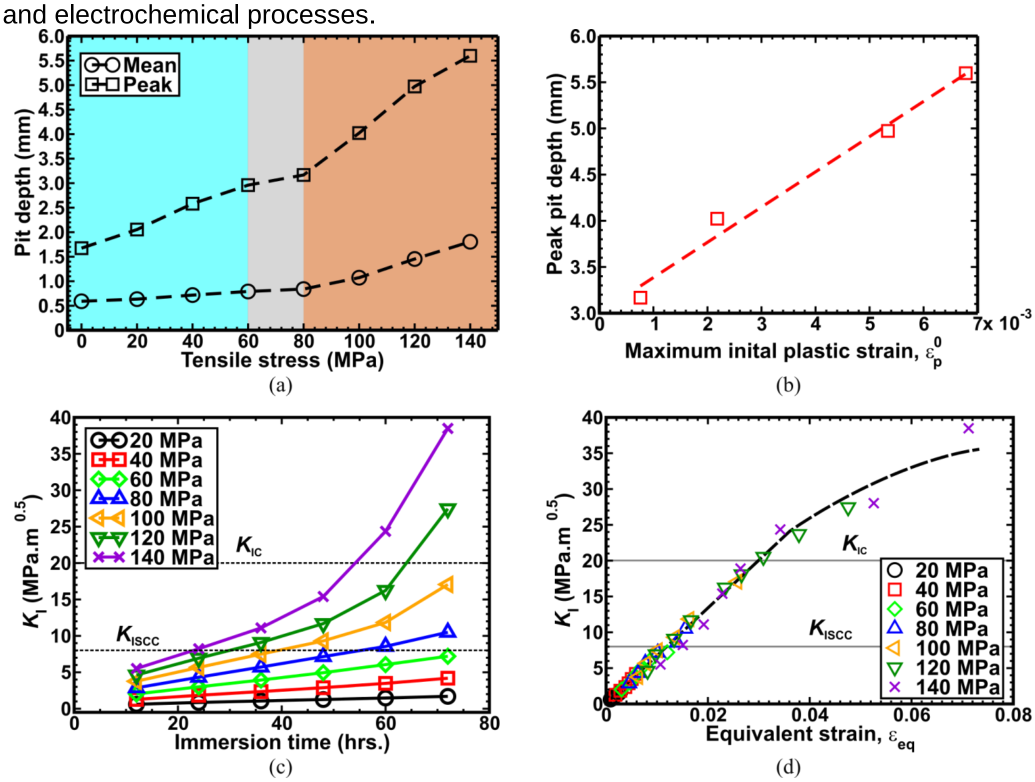

a) The effect of tensile stresses on the observed mean and peak pit depth for the galvanic couple after 3 days of immersion. b) The effect of initial plastic deformation on the observed peak depth. c) The effect of tensile stress on the evolution of stress intensity factor ahead of the corrosion pit. d) The stress intensity factor observed ahead of the corrosion pit as a function of strain for the various loading conditions.

ROLE OF LOCAL MICROSTRUCTURE AND MICROMECHANICS IN GALVANIC CORROSION

Michael D. Sangid, Purdue University
msangid@purdue.edu
Andrea Nicolas, Purdue University
Alberto Mello, Purdue University

Key Words: Galvanic Corrosion, AA7050, Microstructure, Strain Localization, Constituent Particles

Present modeling approaches for galvanic corrosion include theories based on mechanics (relying on stress-state and deformation as the driving force for corrosion) and chemistry (relying on local chemical potentials for the basis of a galvanic reaction), although a unifying platform or set of experiments is needed to directly compare these two methods. In the present work, a set of experiments are conducted that combine chemistry and mechanics approaches in conjunction with simulations of the underlying mechanical behavior of the materials, and the results are used for statistical analyses to view correlations between these disparate techniques. This work includes detailed characterization of the material's grain structure via electron backscatter diffraction (EBSD) and constitutive particles through energy dispersive spectroscopy (EDS), followed by creation of strain maps relative to the microstructure during loading from digital image correlation (DIC), and subsequent galvanic corrosion as spatially measured from a confocal microscope or optical profilometry. As shown in Fig. 1, this is performed spatially across the same region of interest on a specimen. Detailed statistical analyses, based on Gaussian Process modeling, are used to identify spatial locations of corrosion relative to microstructural features and high strain.

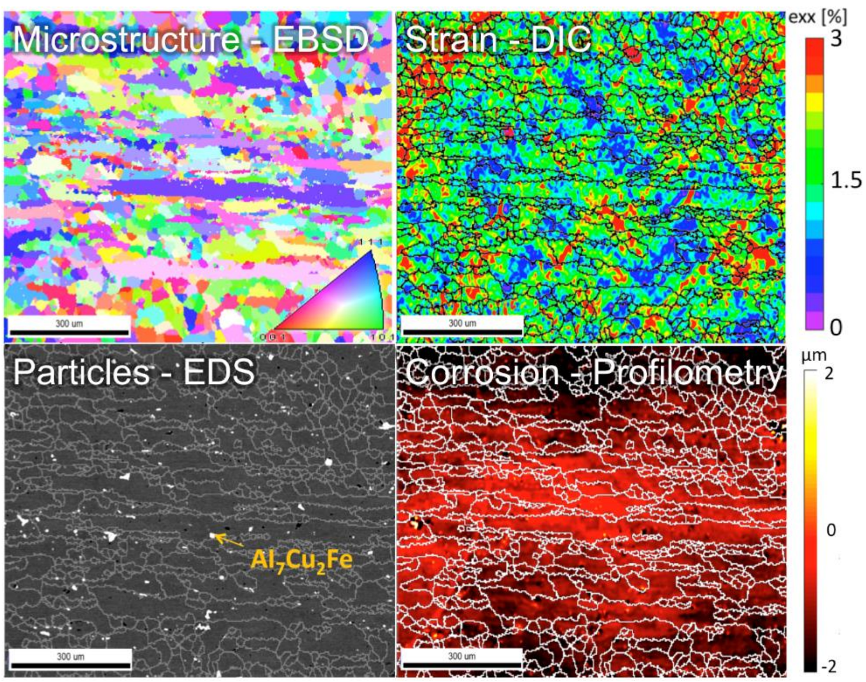

Figure 3 – Experimental characterization for a region of interest of a pre-strain specimen subjected to a galvanic environment.

Strain localization is viewed in various orientations of highly textured AA7050 rolled plate and compared with the results of simulations. To identify the role of the sub-surface microstructure, a similar procedure is performed on columnar AA7050 material, as well as simulated sub-surface grain structures. A detailed galvanic corrosion procedure is followed on pre-strained samples, in which the localized corrosion is tracked every 24 hrs for 20 days. The results show that highly localized strain is not a sufficient condition for corrosion of constituent particles. Yet, a cracked particle resulting in the highest strain accumulation provided the largest corrosion pit. The experiments were repeated on several additional specimens, in which the samples were subjected to a galvanic environment under loading, to segment the driving force for galvanic corrosion as stress-mediated versus strain-mediated. The results will be discussed during the presentation.

Finally, in collaboration with Prof. J. Burns and N. Co of the University of Virginia, the surface topologies of specimens that have been exposed to a galvanic environment are characterized via tomography. Afterwards, the specimens were cyclically loaded to identify the location of crack initiation. Using crystal plasticity simulations, virtual instantiations of the microstructures and specimen's morphologies are created, in order to identify the root cause of crack initiation and potential driving force for short cracks, using a series of fatigue indicator parameters.

EFFECT OF CONFINED ELECTROLYTE VOLUMES ON GALVANIC CORROSION KINETICS IN STATICALLY LOADED MATERIALS

Steve Policastro, Center for Corrosion Science and Engineering, U.S. Naval Research Laboratory
steven.policastro@nrl.navy.mil
Carlos Hangarter, Center for Corrosion Science and Engineering, U.S. Naval Research Laboratory
Rachel Anderson, NRC Post-doctoral Fellow at the U.S. Naval Research Laboratory
Fritz Friedersdorf, Luna Innovations, Inc.

Key Words: Galvanic corrosion, atmospheric corrosion, aluminum, stainless steels

This work investigates the effects that the confined volume of atmospheric electrolytes has on the galvanic corrosion kinetics of martensitic stainless steel alloys coupled with UNS A97075 in simulated atmospheric environments at relative humidity values that span the range of operational exposures. Restricted volumes found in thin films and droplets have been shown to control reduction reaction kinetics and are an ongoing challenge to characterize and standardize . This, along with the dynamic and high concentration of aggressive ions found in confined electrolytes, creates a unique corrosion system that requires a multifaceted approach to evaluate varied conditions, compare them with traditional measurements and more accurately predict galvanic atmospheric corrosion. In this work, corrosion currents in galvanic couples were obtained under three environmental conditions:

1. Bulk electrolytes, in a standardized test configuration, with chemistries relevant to atmospheric electrolytes
2. Thin electrolyte films formed using the Luna test cell and equilibrated at a given temperature and relative humidity
3. Deliquesced droplets formed and equilibrated at multiple temperature and relative humidity values.

In addition, the corrosion currents for the same galvanic couple specimens were evaluated, using an NRL-developed experimental approach, under droplet electrolytes while statically loaded, as shown in Figure 1. These corrosion currents were then compared to the currents obtained from the unloaded conditions.

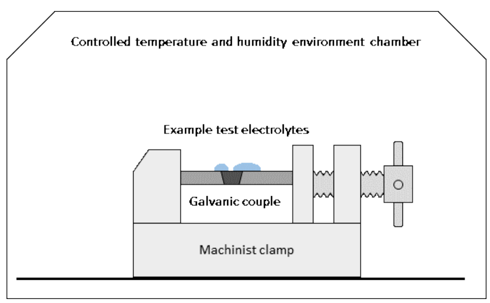

Figure 1 Test set-up for measuring galvanic corrosion currents on statically loaded galvanic couples.

INVESTIGATION OF SCC OF HIGH STRENGTH ALUMINUM ALLOYS BY MEANS OF SLOW STRAIN RATE TEST AND CYCLIC ANODIC POLARIZATION IN COMBINATION

Monica Trueba, Independent scientist
monica.trueba@unimi.it, mokatrueba@gmail.com
Guido Russo, Università degli Studi di Milano, Italy
Stefano P. Trasatti, Università deli Studi di Milano, Italy
Sergio Lorenzi, Università deli Studi di Bergamo, Italy
Marina Cabrini, Università deli Studi di Bergamo, Italy
Antonietta Loconte, Politecnico di Milano, Italy

Key Words: SCC, Al alloys, slow strain rate, electrochemistry.

The stress corrosion cracking (SCC) behavior of high strength 7075-T6 and 2024-T3 Al alloys in NaCl solutions is investigated by means of slow strain rate test (SSRT) and cyclic anodic polarization in combination. Smooth, dog-bone shaped flat tension test specimens, having gage section areas of 40 mm^2 and 32 mm^2, respectively, and 90 mm of gage length, were machined in the longitudinal (rolling) direction from the commercial wrought sheets (Aviometal Spa). The tensile test was performed at a constant strain rate ($\dot{\varepsilon}$ = 10^{-7}, 10^{-6} or 10^{-5} s^{-1}) from a pre-load of about 5 kN until fracture. The electrochemical system consisted in non-connected two Plexiglas cylindrical cells that were fixed at the middle of the opposite surfaces of the tensile specimen (working electrode, surface area at each side of 2 cm^2). The variation of the open circuit potential (OCP) during straining was measured with respect to saturated calomel reference electrode (SCE) by connecting the two electrode system to a Gamry potentiostat. Contemporarily, the opposite surface was electrochemically perturbed by imposing consecutive cyclic anodic polarizations with open circuit potential measurements in between (OCP/polarization sequences), using an Ir-coated Ti auxiliary electrode, another SCE and a second Gamry potentiostat. At least two combined experiments for each test condition were carried out for repeatability check. Experiments with no OCP/polarization sequence during straining, and vice versa, were performed for reference purposes.
The stress-strain curves of Al 7075-T6 (Fig. 1a) show that the ultimate strength and failure strain decrease in aggressive environment as the strain rate is lowered, regardless the electrochemical perturbation, being in agreement with reported data [1]. More interestingly, quasi-periodic stress relaxation/recovery events above the elastic region in correspondence with the dissolution/repassivation cycle were detected for $\dot{\varepsilon} \leq 10^{-6}$ s^{-1} and 0.1667 mV/s of potential scan rate (n). The resolved negative spikes in the stress time derivative curve and the related polarization curves (as log | I | - t) for $\dot{\varepsilon} = 10^{-7}$ s^{-1}, 0.6 M NaCl and n = 0.1667 mV/s are reported in Figure 1b. The spike pattern along the time axe was dependent on $\dot{\varepsilon}$ and NaCl concentration. The results from ongoing combined experiments with Al 2024-T3 for verification of the above findings will be presented altogether with empirical data analysis for a quantitative insight into the environmentally assisted failure mechanisms.

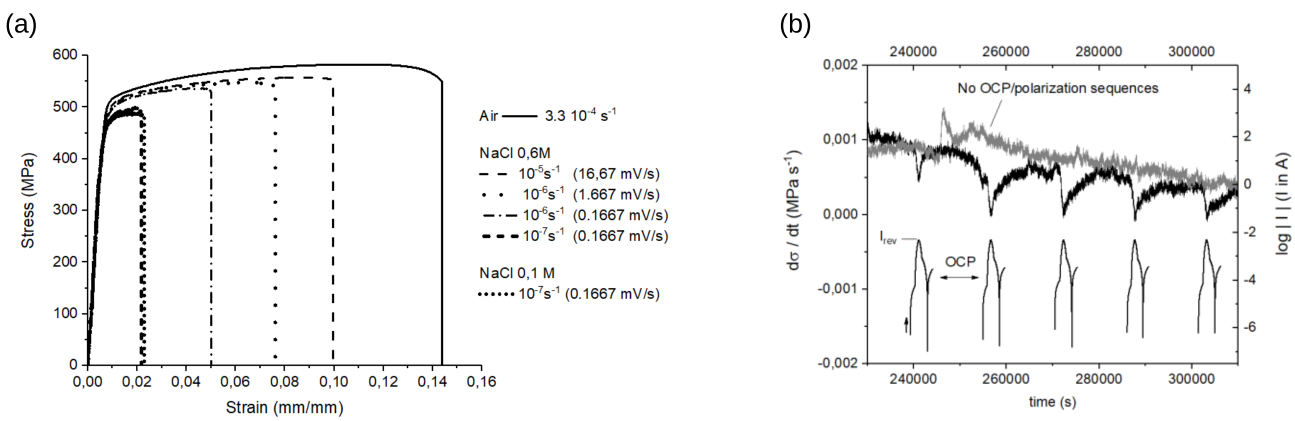

Figure 1: (a) Stress – strain curves of Al 7075-T6 in laboratory air and in NaCl solutions during consecutive OCP/polarization sequences for different $\dot{\varepsilon}$ and n; (b) Stress time derivative curves (above the elastic limit, Fig, 1a) for 0.6 M NaCl and 10^{-7} s^{-1} without and with consecutive OCP/polarization sequences (n = 0.1667 mV/s and the log |I| - time curves for the latter test condition (the arrow indicates the direction of the potential scan and I_{rev} the anodic current limit of the forward scan).

[1] R.E. Ricker, E.U. Lee, R. Taylor, C. Lei, B. Pregger, E. Lipnickas, Metall. Mater. Trans. A 44 (2013) 1353.

INITIATION AND FINAL FAILURE VIA ENVIRONMENTALLY ASSISTED CRACKING IN HIGH STRENGTH ALUMINIUM

T L Burnett, School of Materials, The University of Manchester, Manchester, UK
timothy.burnett@manchester.ac.uk
N J H Holroyd, Department of Materials Science and Engineering, Case Western Reserve University, USA
V C Gudla, School of Materials, The University of Manchester, Manchester, UK
P J Withers, School of Materials, The University of Manchester, Manchester, UK
M Seifi, Department of Materials Science and Engineering, Case Western Reserve University, USA
B C Palmer, Department of Materials Science and Engineering, Case Western Reserve University, USA
J J Lewandowski, Department of Materials Science and Engineering, Case Western Reserve University, USA

Environmentally assisted cracking (EAC) is particularly important to understand and control in high strength aluminium used in engineering applications as moist air provides a suitable environment to assist cracking in these materials. Propagation of EAC has been widely investigated but initiation has been difficult to follow due to it's stochastic nature. We show that time-lapse 3D imaging using X-ray computed tomography offers a way to survey large surface areas whilst maintaining site specific high resolution information giving new insights into this process. In addition the final failure of these materials occurs when the environmentally assisted cracks of intergranular or transgranular type grow to a critical length from the initiation sites. We show through mechanical testing assessment and high resolution fractography that the rapid fracture that follows is also assisted by the environment leading to reduced ductility during the final failure.

Examples from AA5083-H131 and AA7085-T7651 are shown which appear to show the same general behaviour. Round dog bone specimens prepared in the Short Transverse direction were subjected to slow strain rate testing (SSRT) at different strain rates and in different environments. Samples were also pre-exposed to different environments to introduce small corrosion sites to act as 'realistic' stress raisers in the specimens.

MULTISCALE CORRELATIVE CHARACTERIZATION OF ENVIRONMENTALLY ASSISTED CRACK INITIATION, PROPAGATION AND FAILURE IN A HIGH STRENGTH AA5083 H131 ALLOY

Visweswara C Gudla, School of Materials, University of Manchester, Manchester, UK
vcgudla@manchester.ac.uk
Timothy L Burnett, School of Materials, University of Manchester, UK
N J Henry Holroyd, Department of Materials Science and Engineering, Case Western Reserve University, USA
Benjamin C Palmer, Department of Materials Science and Engineering, Case Western Reserve University, USA
John J Lewandowski, Department of Materials Science and Engineering, Case Western Reserve University, USA
Philip J Withers, School of Materials, University of Manchester, UK, M13 9PL

Key Words: X-Ray CT, AA5xxx, Environmental Assisted Cracking, IGC, Electron Microscopy.

Environmentally assisted cracking in a high strength AA5083 H131 alloy has been investigated using a multiscale correlative characterization approach to understand the surface intergranular corrosion to environmentally assisted crack (EAC) transition. Time-lapse 3D synchrotron X-ray tomography was employed during slow strain testing of a sensitized AA5083 sample sensitized at 80 °C for 250 h. In addition, several of the specimens tested were pre-exposed to a chloride containing environment to induce corrosion sites which could act as ‘realistic’ stress raisers in the subsequent straining. Reconstructed volumes of the X-ray CT time-lapse series allowed us to track and follow crack propagation in the material during slow strain rate testing at high resolution <5 µm. Volumes of interest from the test samples identified from the X-ray CT reconstructions were further analyzed post-mortem using electron microscopy and spectroscopy based techniques to study the presence and chemistry of secondary phases such as those based on Mg-Si, and their role in the initiation, propagation and/or arrest of crack tips/fronts.

INTERNAL STRESS AFFECTING ENVIRONMENTAL FATIGUE OF 7075-T651 ALLOY

A.K. Vasudevan & K.Sadadnanda
TDA Inc, Falls Church, VA

N.Chawla, ASU, AZ

Load history has been known to affect fracture and stress corrosion behavior. The degree to which it affects depends on the severity of the load history. It is known that shop peening can retard the SCC lives markedly in steels. Similarly, prestraining can reduce the KIscc and plateau velocity in high strength steels.

These types of experiments are difficult to quantify their effects on the SCC behavior. One can analyze the prestarining effects in a better way by analyzing the effects of single overloads followed by constant applied load to study the behavior. Such experiments can be done by observing the 'incubation time' for a crack to initiate in a fatigue pre-cracked sample, at various constant applied loads in a chemical environment. Such experiments have been conducted on a 7075 aluminum alloy for both static and cyclic loads. It is observed that results are similar in behavior. The data indicates the overall behavior can be analyzed by suggesting that the total stress at the crack tip is related to the contributions from chemistry of the environment and an additional factor from "internal stress" that comes from pre-strain. Hence, we can describe the crack initiation & growth criteria in terms of:

$$\mathbf{K_{Iscc} = K_{applied} + K_{internal\ stress} + K_{environment} > K_{threshold}}$$

Such trends in the behavior, has been observed in pre-strained steel alloys prior to environmental exposure. The general behavior suggests that the internal stress affects the threshold K_{Iscc} more than the plateau velocity. The general SCC behavior is affected by both chemistry and internal stress under external static or cyclic loads.

UNDERSTANDING CORROSION FEATURES AND ALLOY MICROSTRUCTURE EFFECTS ON FATIGUE INITIATION OF CORRODED AA7050-T7451 USING DATA SCIENCE

Noelle Easter Co, University of Virginia
ncc2bf@virginia.edu
Donald Brown, University of Virginia
James Burns, University of Virginia

Key words: Aluminum, corrosion, fatigue, crack initiation, data science

Aluminum alloy 7050-T451 is generally used in aerospace structure due to its high strength-to-weight ratio and high toughness. Local galvanic coupling set up by wicking of electrolyte in between the stainless steel fastener used in the aircrafts and the aluminum substructure promote corrosion of AA7050-T7451. Fatigue crack initiation tend to occur on discontinuities in the aluminum alloy such as the corrosion damage created by the galvanic coupling. Previous study indicate that the individual metrics analyzed for the macro-scale (>250 μm) corrosion features such as pit depth, pit density, pit volume, area of the pit mouth, do not fully correlate to the location of the fatigue crack initiation [1]. The objective of this study is to verify if there is an interaction effect on the metrics analyzed using the macro-scale corrosion damage features using data science techniques. Another objective of this study is to determine if the micro-scale (<250 μm) corrosion features and the alloy microstructure play an important role in the fatigue initiation mechanism of AA7050-T7451.

In order to understand the mechanism governing the fatigue crack formation, corrosion damage mimicking the galvanic coupling effect of AA7050-T7451 and SS316 are artificially created on the surface of AA7050-T7451. A small area on the LS surface of the fatigue specimens are exposed to different environmental conditions to create four different corrosion morphologies, namely, shallow and deep discrete pits, fissures and general corrosion with surface recession. These corrosion morphologies are characterized using the optical microscope, white light interferometer, scanning electron microscope and X-ray computed tomography. The specimens are subjected to fatigue loading using a special loading protocol that creates marker bands on the fracture surface. The specimens are cyclically loaded along the L-direction with σ_{max} of 200 MPa, R ratio of 0.5 at a frequency of 20 Hz. The fatigue testing is done at 23°C and a controlled moist environment with >90% relative humidity during the entire test. After fatigue testing, the fractographs of the specimens are obtained using the SEM. The marker bands from these fractographs are analyzed to calculate the crack growth rate and the fatigue initiation life to create a 10 μm crack from the initiation point are estimated.

Data science approaches are employed to analyze the interaction effect of the individual metrics reported in the macro-scale corrosion feature analysis. Random forest and logistic regression modeling show that there is minimal significance between the macro-scale corrosion feature predictor variables and the fatigue crack initiation points. Even though data science indicate that these factors have less significance, these factors should not be neglected. The micro-scale corrosion features and the distribution of secondary phase particles as well as the grain character are individually analyzed and correlated to the location of the fatigue crack initiation for all the corrosion damage morphologies. Results show that these individual metrics does not fully dictate the location of the fatigue crack initiation. Future work of this study involves the use of data science techniques to understand the relationship between the micro-scale corrosion features, their possible interaction with the alloy microstructure, and the fatigue crack formation. This study will provide understanding on what governs the fatigue crack initiation and inform current micro-mechanical models to incorporate effects of pertinent parameters in predicting remaining life of corroded specimens.

Reference:

[1] Co NEC, Burns JT. Effects of macro-scale corrosion damage feature on fatigue crack initiation and fatigue behavior. Int J Fatigue 2017;103:234–47. doi:10.1016/j.ijfatigue.2017.05.028.

TRANSITION FROM SMALL TO LARGE CRACKS IN TI-6AL-4V SPECIMENS

Sergio Baragetti, Centro per la Gestione dell'Innovazione e del Trasferimento Tecnologico, Via Salvecchio 19, 24129, Bergamo, Università degli Studi di Bergamo - Dipartimento di Ingegneria, Dalmine (BG)
sergio.baragetti@unibg.it
Emanuele Vincenzo Arcieri, Centro per la Gestione dell'Innovazione e del Trasferimento Tecnologico, Via Salvecchio 19, 24129, Bergamo (BG)
Emanuele Borzini, Machine Designer, Via Lagrange 26, 28100 Novara (NO)
A. K. Vasudevan,TDA Inc, Falls Church, Va, USA

Key Words: Ti-6Al-4V, static & cyclic loads, inert & NaCl environments, Kitagawa plots, small & large cracks.

Light alloys allow us to have light components with interesting mechanical features. Ti-6Al-4V is a bimodal titanium alloy employed in aerospace, automotive, maritime and biomedical applications. This alloy has also a good corrosion strength which can be reduced by damages on the passivating surface layer. These damages can be due to an inadequate adhesion of the surface layer, variable loads and interactions with aggressive media [1,2].

For these reasons, quasi-static and fatigue tests on Ti-6Al-4V specimens in different inert, aggressive and very aggressive environments were carried out in the past. Air, air + beeswax coating, paraffin oil, 3.5wt.% NaCl-water solution and water-methanol solutions with several percentages were investigated in order to evaluate the chemical and mechanical forces of the corrosion fatigue phenomena [3].

Stress corrosion cracking (SCC) tests on a low strength steel [4] showed that the threshold of dJ/dt decreases with decreasing deformation rate and that the electrochemical energy contribution on the crack growth is independent from the displacement rate but dependent from the electrochemical conditions at the crack tip.

As stated in [5] the crack size effect must be considered because small cracks have very high growth rate. Slow strain rate tensile and low-amplitude cyclic tests on micro-notched high strength low alloy steel specimens showed that crack growth strongly depends on the notch-tip plastic zone and hydrogen activity itself. High cycle fatigue tests with different notch shapes showed in [7] that the maximum stress and gradient increase with decreasing defect size. The stress state at the notch root is a function of the geometry. In [7] an elasto-plastic FE modelling with a multiaxial fatigue criterion and a correction for the stress gradient is also shown. Tanaka et al. [8] applied the fracture mechanics approach to fatigue crack initiation for also small notch-tip radius. In [9] micro-notched 316L steel specimens in a chloride medium gave the crack propagation rate in function of the global loading. A FE model was also developed in [9].

Micro-notched Ti-6Al-4V specimens were machined to get various notch lengths (up to about 100 μm) & tested under static & cyclic loads to obtain fracture properties, incubation times. The notches were made using Electro Discharge Machining (EDM) in order to reach various values of stress concentration factor (K_t) without notch tip plasticity.

The tests were carried out on a testing machine previously designed by the Structural Mechanics Laboratory (SM-Lab) of the University of Bergamo and now modified so that bigger specimens can be used and easier setting can be reached. During the tests an axial load was applied with a fixed increment of it every fixed time. The machine has specific grips in order to avoid unwanted bending moment on the specimens.

Test results are plotted on Kitagawa diagram to analyze the role of environment on static and cyclic applied loads. At the threshold i.e. at the endurance limit (horizontal line in Kitagawa diagram) we calculated:

$$K_{max}^{th} = \sigma_{max}^{end}(\pi a)^{\frac{1}{2}}.$$

[1] Brown B.F. 1972: 147–244, Naval Research Laboratory, Washington, D.C.
[2] Lee E.U., Vasudevan A.K., Sadananda K. International Journal of Fatigue 2005; 27: 1597-1607.
[3] Baragetti S., Villa F. Fracture and Structural Integrity 30 (2014), 84-94.
[4] Sarioğlu, F. and Doruk, M. Conf.Proc., Advances in Fracture Research (ICF-7), Houston, Texas, USA, ed. K. Salama, 1989, 1, pp. 259–65.
[5] Gangloff RP. Met Trans A 1985;16A (5):953-69.
[6] Bosch, C., Delafosse, D., Longaygue, X. European Corrosion Congress 2010 (Eurocorr2010), Sep 2010, Moscou, Russia. 2, pp.1558-1570, 2010.
[7] Franck Morel, Anne Morel, Yves Nadot. International Journal of Fatigue,Elsevier, 2009, 31 (2), pp.263-275.
[8] Tanaka K., Nakai, Y., Kawashima, R. Engineering Fracture Mechanics 18, 5, pp.1011-1023,1983.
[9] Tinnes, J.P., Delafosse, D., Bosch, C., Raquet, O., Santarini, G. Euroorr 2004.

A CONTINUUM MECHANICS MODEL FOR FATIGUE LIFE PREDICTION WITH PRE-CORROSION AND SEQUENTIAL CORROSION FATIGUE

Mehdi Amiri, Technical Data Analysis Inc., Falls Church, VA
mamiri@tda-i.com

Key Words: Pre-corrosion, Fatigue, Sequential corrosion-fatigue, Continuum mechanics.

We present a continuum model to predict pre-corrosion fatigue which is a prevalent damage mechanism in aerospace structures under operational conditions. It is assumed that the process of corrosion and fatigue sometimes exist separately to a large extent. In this scenario, it is assumed that when an aircraft is in fight at high altitude, cyclic loading due to engine vibration and flutter is at its maximum, whereas the corrosive processes due to moisture or temperature are minimal. And when the aircraft is on the ground the corrosive process is at its maximum, whereas vibration loading is non-existent. For demonstration purposes, we study the effect of prior corrosion on fatigue life of aluminum alloy 7075-T6. In this work, we employ Continuum Damage Mechanics (CDM) as the modeling platform to study the fatigue crack initiation and growth from a pre-existing corrosion pit. In the CDM approach, a crack is assumed to initiate when damage variable, D, attains a critical value D_c. We use the corrosion-free fatigue data to calibrate D_{c0} for 7075-T6. This value for critical damage signifies the failure of a representative value element (RVE) when corrosion is non-existent, see Fig. 1. In other words, the corrosion exposure time is zero, $t = 0$. The corrosion RVE starts to corrode as time elapses. The effect of corrosion is shown by increased in surface roughness. At initial times of exposure, damage occurs as corrosion pits and increased surface roughness. As time passes, pits grow in size and spread over the entire surface of RVE. After long time of exposure, the RVE will corrode in a self-similar manner, meaning that we assume that surface roughness reaches a limit value while uniform surface recession continues. We refer to this model as the concept of corroded RVE as shown in Fig. 1. We used this model to predict the fatigue life of 7075-T6 exposed for 0, 96, 768 and 1536 hrs in the prehesion spray. The predicted results are in a reasonable agreement with experimental data. We further tested the model for life prediction of sequential corrosion-fatigue scenarios where corrosion and fatigue occur in sequence. For maximum stress of σ_{max} = 340 MPa, load ratio of R = 0.1 and exposure time of t_{exp} = 100 hrs, the model predicts 17% increase in fatigue life for sequential corrosion-fatigue than the pre-corrosion fatigue. This result is interesting since it shows the interaction between corrosion and fatigue cycles. The result infers that if the corrosion time is spread over the fatigue cycles the life may increase.

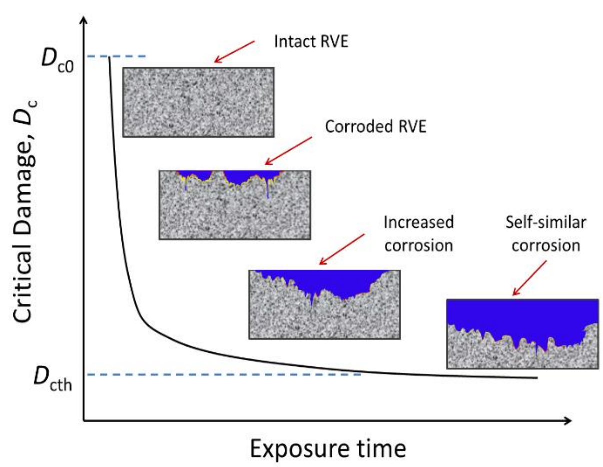

Figure 4 – A schematic that shows the concept of corroded RVE. The critical damage changes from D_{c0} for un-corroded RVE to D_{cth} for self-similar corroded RVE.

4D MICROSTRUCTURAL AND ELECTROCHEMICAL CHARACTERIZATION OF DISSIMILAR-METAL CORROSION IN NAVAL STRUCTURAL JOINTS

S. Niverty, Center for 4D Materials Science, Arizona State University, USA
T. Stannard, Center for 4D Materials Science, Arizona State University, USA
J. Graber, Center for 4D Materials Science, Arizona State University, USA
J.J. Williams, Center for 4D Materials Science, Arizona State University, USA
N. Chawla, Center for 4D Materials Science, Arizona State University, USA
X. Xiao, Advanced Photon Source, Argonne National Laboratory, Argonne, IL
F. De Carlo, Advanced Photon Source, Argonne National Laboratory, Argonne, IL

Key Words: Corrosion, Galvanic, X-ray tomography, Potentiodynamic polarization, FIB-SEM

Dissimilar metal corrosion in aircraft and naval structures has proven to be a persistent challenge. Decades of research in the area have shown that such complex contact surfaces are subject to a combination of corrosive environments and mechanical loads. Hence, this multi-faceted problem must be understood from electrochemical, microstructural and mechanical standpoints to comprehensively understand corrosion damage in these systems.

In this work, we have focused on studying corrosion in a dissimilar metal couple consisting of an Al7075-T651(plate with threaded/unthreaded holes) anode and Ti-6Al-4V cathode(screws/rivets). Synchrotron X-ray tomography was used to perform *in situ* corrosion fatigue experiments on the dissimilar metal couple specimen in a 3.5 wt% NaCl environment to gain insights on the corrosion assisted crack initiation and propagation process.
The evolution of microstructure during the accelerated corrosion of bare Al7075-T651 in a 3.5 wt.% NaCl environment was also investigated. Interrupted Tafel testing was used to understand the evolution of corrosion and pitting on the alloy surface at each stage of the experiment. Additionally, the role of grain boundaries and a variety of second phase particles with their associated changes in morphology was studied. A confluence of methods comprising potentiodynamic polarization, X-ray microtomography and the FIB-SEM have been used.
Our latest efforts in this area attempt to incorporate diffraction contrast tomography(DCT) to study corrosion behavior in Al7475. The technique is akin to 3D EBSD and allows us to investigate the role that grain boundaries, triple points and inclusions can have on the initiation and propagation on pitting.

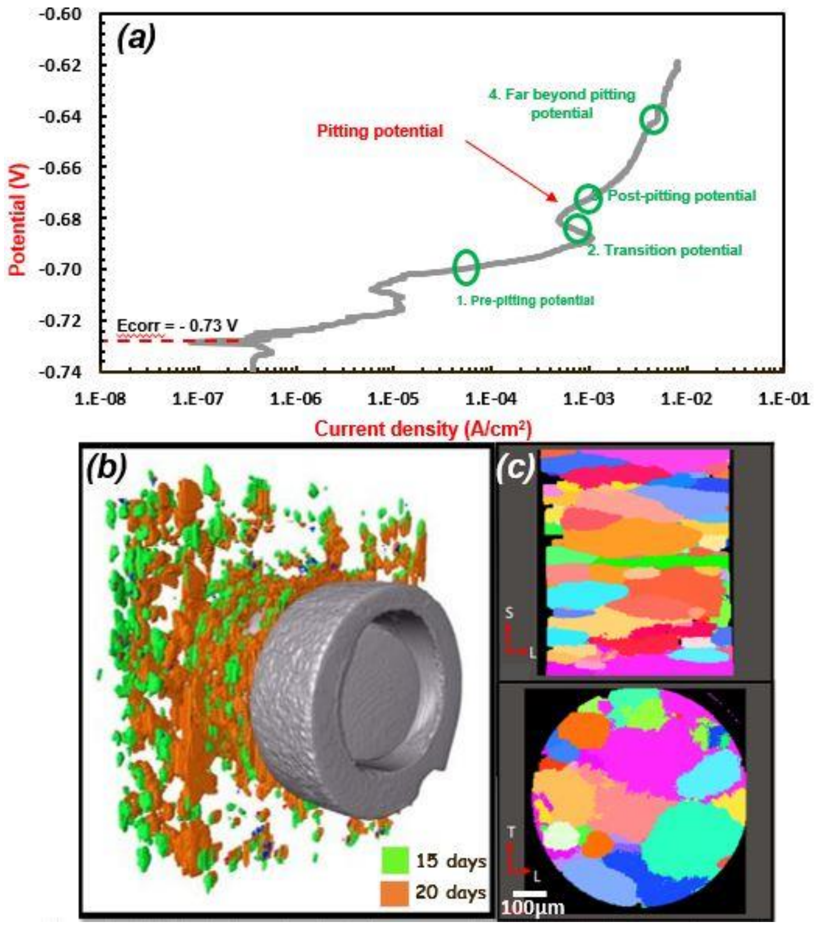

Figure 1:(a) Potentiodynamic polarization curve of Al7075-T6511 showing regions where the experiment was interrupted, (b) Pitting corrosion in Al7075-T651/Ti-6Al-4V couple after 15 and 20 days of immersion corrosion in 3.5 wt.% NaCl solution, (c) DCT of Al7475 showing 3D grain structure along the SL and TL directions.

ELECTROCHEMICAL AND ENVIRONMENTAL ASSISTED CRACKING BEHAVIOR OF AA2024 T3 AND AA7075 T6 WELDED BY MEANS OF FSW

M.Cabrini, University of Bergamo, Department of Engineering and Applied Science
marina.cabrini@unibg.it
S.Lorenzi, University of Bergamo, Department of Engineering and Applied Science
T.Pastore, University of Bergamo, Department of Engineering and Applied Science
S.Bocchi, University of Bergamo, Department of Management, Information and Production Engineering
G.D'Urso, University of Bergamo, Department of Management, Information and Production Engineering
C.Giardini University of Bergamo, Department of Management, Information and Production Engineering

The paper deals with the stress corrosion behavior of butt joints obtained by friction stir welding (FSW). The experimental study was performed on prismatic specimens obtained from FSWed joints of AA7075-T6 and AA2024-T3 alloy sheets having a thickness equal to 4 mm. The tests were executed on the same alloy (AA7075-AA7075 and AA2024-AA2024) and mixed joints (AA7075-AA2024). Tensile tests and four-point bending tests were carried out to evaluate the corrosion behavior and stress corrosion cracking susceptibility of FSW joints. During the tests, the electrochemical behavior of both the loaded (80% of the yield strength) and unloaded specimens in 3.5% NaCl solution was monitored by means of corrosion potential measurement, and electrochemical impedance spectroscopy (EIS). In the first hours of dipping, the EIS spectra of the loaded specimens of AA2024-T3 were different from the unloaded ones. After 24 hours, the electrochemical response became the same for all the specimens. This behavior was attributed to the formation of a thick layer of corrosion products that hindered the electrochemical couple within the specimens. After 1500 hours of immersion, the loaded specimens showed an intense intergranular attack which was not observed on the unloaded specimens. This stress enhanced intergranular attack was observed in the nugget of the welding, close to the continuous copper-rich precipitates at the recrystallized grain boundaries, induced by the thermo-mechanical action of the welding tool. These precipitates were formed of the coalescence of sub-micrometric precipitates present in the naturally aged base metal. Intergranular attacks were not observed in the heat-affected zone and on the base metals – where grain recrystallization did not occur. In these zones, the presence of sporadic shallow pits was only observed in correspondence of the large copper rich precipitates. The loaded specimens of AA7075-T6 showed EIS spectra different from the unloaded ones, in particular, the un-stressed specimens had three phase constants, whereas the stressed only two. The third phase constant at high frequencies disappears as the time of dipping increased, and the EIS spectra of all the specimens became similar. At the end of the tests, all the AA7075-T6 specimens – stressed and un-stressed - showed a very intense exfoliating attack started from the heat affected zone and propagated along the rolling direction. On the four-point bending specimens it was not possible to evidence the effect of the load on the morphology of the attacks. Finally, in the first hours of immersion, the EIS spectra of the AA7075-AA2024 welds showed EIS spectra similar to those of the AA2024-T3, increasing the dipping time, the EIS spectra became similar to the AA7075-T6 ones. Independently from the stress applied on these specimens, the corrosion morphology, was located only on the AA7075-T6 side.

The complex behavior of the considered welds was also evidenced by means of local open circuit potential (LOCP) measurements: in fact, it was possible to observe the more active areas located in correspondence of heat affected zone. The differences in the LOCP can be attributed to the changing in the microstructure owing to the thermal mechanical action of the welding. The hardness along the welds showed a similar profile to the LOCP.

EXAMINATION OF FACTORS INFLUENCING FATIGUE CRACK GROWTH IN LEGACY ALUMINUM ALLOYS

Sarah E Galyon Dorman, SAFE, Inc
sgd@saf-engineering.com
Justin W Rausch, SAFE, Inc
Scott A Fawaz, SAFE, Inc

Key Words: chromate, corrosion fatigue, environmentally assisted cracking, atmospheric corrosion, galvanic corrosion

In work sponsored by the Office of Naval Research a corrosion fatigue test method to better replicate real world corrosion conditions using salt film, relative humidity, ozone and UV-light, is being developed [1]. This method is being used to evaluate the effect of atmospheric corrosion conditions in AA7075-T651 with inhibitive coatings including epoxy chromate and three chromate replacement coatings (water and epoxy based rare earth primers and an aluminum rich primer). The corrosion fatigue results are being paired with leaching studies under traditional immersion and atmospheric conditions on the primers to determine how the leaching rates relate to the ability of a primer to inhibit fatigue damage.

Research shows that chromate in concentrations related to leaching rates can slow fatigue crack growth in aluminum alloys in stress ranges relevant to airframe maintainers [2,3]. The fatigue tests showing inhibition with low levels of chromate (0.05 mM) were completed with chromate added to a full immersion sodium chloride solution. It remains unclear if epoxy chromate based and other polymeric inhibitor coatings can affect corrosion fatigue under atmospheric corrosion conditions. The protection provided by corrosion inhibitors undergoing fatigue can be affected by loading conditions (ΔK, frequency) and also likely by the environment due to changes in coating leaching. An improved understanding of how environmental and loading parameters influence a coating's ability to offer protection against corrosion fatigue damage would greatly help the coating community to design more robust coating protection systems.

Another focus area of the ONR sponsored research is in quantifying the corrosion damage to fatigue crack transition. A standardized specimen and testing protocol to evaluate the relative influence of material, environment, inhibitors, loading spectrum and other inputs on the pit-to-crack transition was developed [2,3]. The methodology uses a narrow plate specimen with a centrally located hole with a preferential pit (diameter approximately 150 µm) placed at the corner of the hole; current work is being completed on legacy aluminum alloy AA7075-T651. The plate thickness and hole diameter are consistent with commercial and military airframe applications. The method uses direct current potential drop (DCPD) to measure the crack length. In the current research the test methodology is being transitioned to evaluate galvanic interactions when a fastener of either stainless steel or titanium in placed in the hole. The fastener contact geometry is limited to two boundary conditions either the hole bore and starting pit are bare or only the starting pit is left unprotected. The fastener shank is left unprotected as well. The galvanic potential between the aluminum and the fastener is measured and then used to control the corrosion potential during the corrosion fatigue testing. This method allows for bench top electrochemical tests to be used to control the mechanical testing and also removes the time effect for galvanic corrosion to begin.

The overarching objective of the research is to improve and transition the results on the effect of environmentally assisted fatigue in high performance metallic alloys (crack growth rate data) to the DoD research and depot maintenance activities by integrating all data into the AFGROW fatigue crack prediction software allowing for the inclusion of corrosion damage and environment effects on fatigue crack life predictions. Likewise better methods for coating and material evaluation are being produced.

1 D. Laing, et al., "Effects of Sodium Chloride Particles, Ozone, UV and Relative Humidity on Atmospheric Corrosion of Silver," Journal of the Electrochemical Society, 2012, 157 (4) pp. C146-C156.
2 S.E. Galyon Dorman, J.W. Rausch and S.R. Arunachalam, "Examination and Prediction of Corrosion Fatigue Damage and Inhibition," Corrosion Reviews, ISSN (Online) 2191-0316, ISSN (Print) 0334-6005, DOI: https://doi.org/10.1515/corrrev-2017-0057.
3 S.E. Galyon Dorman, et al, (2016) Managing Environmental Impacts of Time-Cycle Dependent Structural Integrity of High Performance DoD Alloys, SAFE Inc., SAFE-RTP-16-045.

THE INFLUENCE OF DYNAMIC ATMOSPHERIC CONDITIONS ON ENVIRONMENT ASSISTED CRACKING AND CORROSION FATIGUE

Fritz Friedersdorf, Luna Innovations
friedersdorf@lunainc.com
Nathan Brown, Luna Innovations
Brandi Clark, Luna Innovations
Jacob Wright, Luna Innovations

Key Words: Environment-assisted cracking, corrosion fatigue, atmospheric corrosion.

Environment-assisted cracking (EAC) and corrosion fatigue (CF) of aluminum alloys in corrosive atmospheres are significant maintenance and safety issues for aircraft. It is well known that these cracking phenomena result from the combined effects of environment, mechanical loads, and material properties. The service life of an aircraft structure is dependent on various stages of degradation associated with formation of corrosion damage, crack nucleation, and crack propagation. Which of these stages limits the service life may be specific to a given component and can be dependent on a large number of factors, including environmental severity, mechanical loading, and protective coatings. The focus of this research effort is to evaluate the influence of protective coatings on the incubation, nucleation, and growth of cracks under static and fatigue loads using both instrumented double cantilever beam samples and a hydraulically actuated four point bend test system (

Figure ***5***). The capacity of coatings with soluble inhibitors and galvanically sacrificial pigments to influence crack nucleation and growth for short and long cracks is being investigated.

In previous work, it has been clearly demonstrated that crack growth rates are strongly dependent on time variant atmospheric conditions in static load tests where drying processes are much more aggressive than wetting, high humidity, or immersion test conditions. Experimental measurements of current distributions in artificial cracks are consistent with accepted mechanistic models where high oxygen reduction rates at the crack mouth support anodic dissolution, hydrolysis, and acidification within the crack, and subsequent hydrogen reduction near the crack tip. This work on long cracks ($\approx$ 1 mm) using bare AA7075-T6 facture samples is being extended to include the influence of galvanic couples, crevices, and coatings on EAC and CF initiation and propagation (

Figure ***6***). Initial results demonstrate that crevices and galvanic couples, as would be expected at a fastener, reduce the crack nucleation time, and that corrosion fatigue crack propagation also accelerates during drying in cyclic atmospheric corrosion tests. The rate of change of environmental parameters, such as relative humidity, is a significant factor for EAC testing, and static environmental conditions may yield misleading and non-conservative results. These measurement methods and test results may have utility in evaluating EAC mechanisms, quantifying mitigation strategies, and validating predictive models.

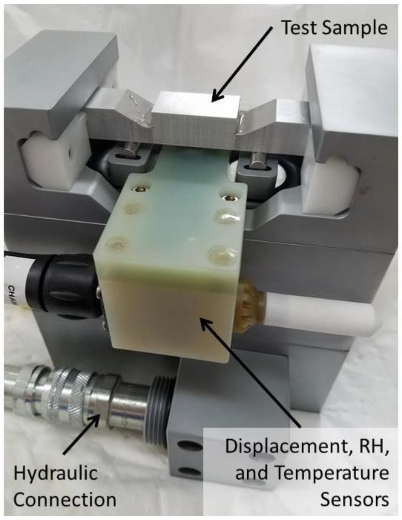

Figure 5 – Corrosion fatigue test apparatus for use in atmospheric corrosion tests.

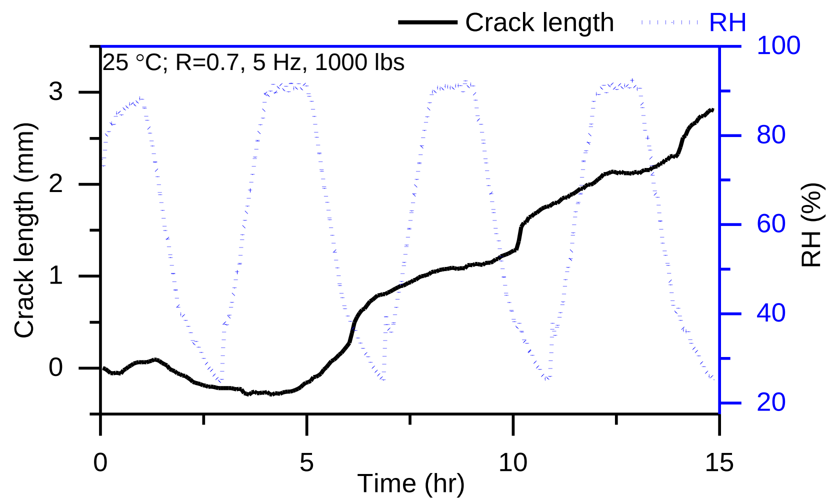

Figure 6 – Corrosion fatigue crack length as a function of time for cyclic humidity test at a constant temperature. Alloy is AA7075-T6 exposed to a simulated sea salt.